This is a repository copy of *Effect of particle shape on flow in discrete element method simulation of a rotary batch seed coater*.

White Rose Research Online URL for this paper:
http://eprints.whiterose.ac.uk/105432/

Version: Accepted Version

Effect of Particle Shape on Flow in Discrete Element Method Simulation of a Rotary Batch Seed Coater

Mehrdad Pasha[1], Colin Hare[1], Mojtaba Ghadiri[1], Alfeno Gunadi[2], Patrick M. Piccione[2]

[1] Institute of Particle Science & Engineering, University of Leeds, Leeds, UK

[2] *Process Studies Group, Syngenta Ltd, Jealott's Hill International Centre, Bracknell,*

Berkshire, UK

*Contact Email: m.ghadiri@leeds.ac.uk

Telephone: +44 (0)113 343 2407

Abstract

In the seed processing industry, rotary batch seed coaters are widely used for providing a protective coating layer (consisting of various ingredients including fertilisers and crop protection chemicals) on the seeds. Seed motion and mixing are important in ensuring uniform coating. In the batch seed coater, the base of a cylindrical vessel rotates, whilst the cylindrical wall is stationary and two baffles turn the bed over for mixing. In the present study, the Discrete Element Method (DEM) is used to simulate the effect of particle shape on motion and mixing in this device. Corn seed is used as a model material and the effect of its shape on motion is analysed by considering two approaches: (1) manipulation of rolling friction to account for shape as it is commonly used in the field; (2) approximation of the actual shape by a number of overlapping spheres of various sizes. The geometry of corn seeds is captured using X-Ray micro tomography and then the ASG2013 software (Cogency, South Africa) is used to generate and optimise the arrangement of the overlapping spheres. A comparison is made of the predicted tangential and radial velocity distributions of the particles from DEM and those measured experimentally. It is concluded that for rapid shearing systems with short collisional contacts a small number of clumped spheres suffices to provide a reasonable agreement with experimental results. Equally well, manipulating the rolling friction coefficient can provide results that match experiments but its most suitable value is unknown a priori, hence the approach is empirical rather than predictive.

1 Introduction

In industries such as agricultural, food, detergent and pharmaceutical manufacturing, granule mixing and coating are common processes. The quality of finished product is strongly influenced by the rate of mixing and quality of coverage, which themeselves depend on the spraying and spreading processes. Hence it is important to understand the effect of each process parameter on the final product quality and to optimise them. To do so, the particle kinematic behaviour (flow field, mixing pattern, etc.) needs to be analysed. Discrete Element Method (DEM) [1] provides a robust way of simulating particulate systems [2–4]. Spherical particles are most commonly used due to the simplicity of contact detection and mechanics, where contact can be detected if the distance between two particles become less than the sum of their radii. This results in efficient contact detection and faster contact force calculations. There are many other approaches for representing particle shape, such as elliptical [5], polygonal [6], bonded assemblies of polygons [7], spherosimplices [8] and super-quadric particles [9]. Lu et al. [10] have recently provided a comprehensive review on approaches for consideration of non-spherical particles in DEM.

To account for the non-sphericity of particles, Morgan [11] proposed a new method for simulating mechanical interlocking of irregularly shaped particles by restricting particles from rolling. This method showed that the addition of rolling friction would lead to more realistic values of bulk friction compared to free rolling spheres. Ai et al. [12] have classified the rolling resistance models into four categories: directional constant torque, viscous, elastic-plastic spring-dashpot and contact-independent models. Wensrich and Katterfeld [13] reported that consideration of rolling friction alone would not lead to an accurate representation of the particle shape in the case of simulating the angle of repose. They

attributed this to the fact that the rolling friction only acted to oppose the rolling motion whereas in reality the non-sphericity of a particle may increase rolling.

Favier et al. [14] implemented a new technique for considering particle shape in DEM, where the particle shape was approximated by a number of overlapping or touching spheres with different sizes (known as clumped spheres), the centres of which were fixed in a position relative to each other. This method approximates the shape of irregular particles by a number of clumped spheres, while maintaining computational efficiency. Theoretically, any particle shape can be modelled, although highly angular particles require a large number of small spheres to approximate their sharp edges, making this method unsuitable [15]. Approximation of shape using this technique produces undesired surface roughness for the modelled particles [16]. However, the induced roughness can be controlled by increasing the number of spheres, though this has a negative impact on the computational efficiency.

Wiącek et al. [17] investigated the influence of grain shape and interparticle friction of peas and beans on the mechanical response of the assemblies in a uniaxial compression test. They showed that the mechanical response of the granules was highly affected by increasing the aspect ratio of the particles; the lateral-to-vertical pressure decreased as the particles aspect ratio was increased. Once the aspect ratio of the particles exceeded 1.6, however, the lateral-to-vertical pressure became relatively invariant. Moreover, the authors reported that the DEM simulations predicted values of the effective elastic modulus of the bed close to those obtained from experiments for spherical particles (i.e. peas) but not in the case of oblong particles (i.e. beans). Hare and Ghadiri [18] investigated the effect of particle shape and roughness of particles on their flowability in a shear box by DEM. The particles were represented by a number of overlapped spheres and the roughness was controlled by the separation of the centres of overlapped spheres from one another. They concluded that an increase in roughness of particles resulted in an increased stress ratio. Gonzalez-Montellano

3

et al. [19] investigated the discharge flow of glass beads and corn seeds from silos using DEM, where the glass beads and corn seeds were simulated using spherical and multiple non-adhesive clumped spheres, respectively. Their predictions for the mean bulk density for the filling phase, discharge time and flow patterns were then compared to the experimental results. The authors reported that due to the shape and difficulty of measuring the friction of irregularly shaped particles, the flow pattern and discharge time in the simulations did not follow those obtained in experiments. Therefore, the value of particle-particle friction coefficient was calibrated using sensitivity analysis based on the approach of Balevicius et al. [20]. More recently, Gonzalez-Montellano et al. [21] investigated the vertical and horizontal distributions of the normal pressure, tangential stresses, mobilised friction and velocity profiles of filling and emptying silos using experiments and DEM. They found a reasonable agreement with experiments. However, the predicted horizontal distribution of normal stress on the wall was greater for the central positions on the wall, as compared to those measured experimentally. The authors suggested hybrid models, similar to the work done by Lu et al. [22], where FEM and DEM were coupled may to improve the results.

Recently, there have been studies carried out on the adequacy of the number of clumped spheres needed to represent particle shape in DEM. At single particle level, Song et al. [23] investigated this for tablet-shaped particles, where the shape was represented by 10, 26, 66 and 178 mono size spheres. They analysed the magnitude of angular velocity of a tablet upon impact on to a stationary tablet. They have reported that for all the cases, no agreement could be found between the simulations and experiments, where the magnitude of the angular velocity was much higher in the simulations. They also reported that increasing the number clumped spheres increased the magnitude of angular velocity of particles upon impact on to another tablet. They attributed this to the fact that there were more sphere contacts when using a larger number of clumped spheres. It should be noted that these findings may not be

4

applicable to clumped spheres representing a bed of particles, since there are more particle-particle contacts in such a system. Similarly, Price et al. [24] investigated the angular velocity of irregularly shaped particles, represented by clumped spheres, upon impact on to a flat steel plate. They reported that increasing the number of clumped spheres did not influence the angular velocity in the case of densely packed spheres, where no voids were present in the structure of the particle. They attributed this to the fact that in the particle shape that they investigated the particle was compact; hence the centroid of the particle was located close to the centre of the particle. It is noteworthy that their simulated particle shape was not highly irregular and the surfaces were smooth; hence further investigation is required for more complex particle shapes. Moreover, the above work only addressed the effect of particle shape at the single particle level. At the bulk level, Markauskas et al. [25] investigated the adequacy of the number of clumped spheres required for DEM simulations in a particle piling system. In their study, an ellipsoid particle shape was approximated using a number of spheres. They reported that the porosity of the bed initially decreased, but remained relatively constant for assemblies consisting of more than 13 clumped spheres. Moreover, the average coordination number of particles increased with the number of spheres used, but again remained relatively constant for particles of consisting of more than 13 spheres. In their work, the simulation results have not been directly compared to experiments; hence it is difficult to assess the accuracy of the predictions. In another work, Kodam et al. [26] investigated the accuracy of shape representation by using clumped spheres and actual cylindrical particle shapes for both single particle and bulk levels. In their work, a cylindrical particle as well as two assemblies of 9 and 54 mono-size clumped spheres were considered. At the single particle level, the particle was impacted on to a flat surface and the angular velocity was analysed. Compared to theoretical results, a poor agreement was found in both cases of clumped spheres (9 and 54 spheres), whereas a relatively good agreement prevailed for the

actual cylindrical particle shape. Moreover, they investigated the residence time of the particles in a baffled rotating horizontal drum, where a reasonably good agreement was found for all the particle shapes investigated (both clumped spheres and actual cylinders). Further analysis of the bulk solid fraction of particles in a cylindrical vessel showed that using 54 clumped spheres slightly underpredicted the solid fraction. This could be as a result of artificial introduction of surface roughness and could be minimised by considering poly-size spheres in the individual particle assembly; where smaller spheres are present at the surface of the particle to improve the accuracy of shape representation. Kruggel-Emden et al. [27] also raised concern on the validity of using the clumped sphere method. They reported that at the single particle level at least the method did not reliably simulate the real case. However, they suggested that the bulk behaviour might not face the same shortcomings. Guo et al. [28] investigated the effect of particle aspect ratio and surface geometry on granular shear flow of rod-like particles in three regimes of solid volume fractions (i.e. dilute, intermediate and dense regimes).

Much work has been carried out in the literature on consideration of particle shape in DEM simulations. In most cases, the adequacy of the number of clumped spheres required to reliably simulate the real case is investigated at the single particle level, which may not represent bulk behaviour of particles. In this paper however, we report on our work on the effect of particle shape on particles motion in a rotary batch seed coater, using both spherical particles with the addition of rolling friction, and particles represented by clumped spheres and, comparing the simulation results with those obtained experimentally.

2 Materials and Methods

2.1 Experiments

A series of laboratory experiments were conducted using a SATEC ML2000 rotary batch seed coater (0.3 m in diameter and 0.21 m in height) as shown in Figure 1. For the seed coating, a liquid stream is introduced by a nozzle to a spraying disc, where the liquid is atomised and sprayed onto the surfaces of the seeds. The base rotates to mobilise the seeds, whilst the vertical plates act as baffles, turning the bed over and ensuring adequate mixing of the seeds in order to increase the uniformity of the seed coating. In the work reported here the system was run dry, i.e. no liquid was added during the experiments. The interest here is in corn seeds, which are used as the test material. The seeds are sieved prior to the experiments and only particles in the range of $7.1 - 8.0$ mm are considered. For both simulations and experiments, the base rotational speed is 300 rpm, the baffle angle is $45°$ and the baffle to wall clearance is 15 mm. The motion of particles moving on the bed surface near the vertical baffles is captured using a Redlake HG-100K high-speed video recorder, where the velocities in the x and y directions are calculated from the distance travelled by each particle within one video frame (4 ms) in the measurement cell (50 mm by 50 mm) highlighted in Figure 2. The tangential and radial velocity of particles are then calculated using Equations 1 and 2.

$$V_{\theta} = V_x \sin(\theta) + V_y \cos(\theta) \qquad\qquad \text{Eq.(1)}$$

$$V_r = V_x \cos(\theta) + V_y \sin(\theta) \qquad\qquad \text{Eq.(2)}$$

where V_x and V_y are velocities in x and y direction, respectively, and θ is the angular position of the particle (anti-clockwise from the x-axis).

2.2 DEM Simulations

A series of DEM simulations were carried out using the EDEM® software (DEM-Solutions, Edinburgh, UK) by considering the rolling friction to account for non-sphericity of particles, and also approximating the shape by clumping a number of spheres with various sizes. The effect of particle shape is presented in terms of the radial and tangential velocity distributions of particles inside two cubic measurement cells in the seed coater as shown in Figure 3. The length of each side of the cubic measurement cell is 50 mm (approximately seven particle diameters). In these DEM simulations, the motion of particles in the absence of coating liquid is considered since the main interest is the bulk motion and its sensitivity on the coefficient of rolling friction. The simulations were conducted using Hertz-Mindlin contact model [29] with rolling friction based on viscous dissipation [30] where the size of vessel and particles are the same as those used in the experiments. A bed consisting of 4,200 particles corresponding to 1.2 kg of corn seeds was used. The simulations were carried out using a constant rotational speed of the base at 300 rpm for 25 s of process time. The elastic modulus of particles was reduced by two order of magnitude in order to speed up the simulations. This was considered to be appropriate since the motion of non-adhesive particles was of interest. It has been shown that varying elastic modulus to this degree is not influential on the flow patterns generated [22 - 23]. Coefficients of restitution and sliding friction of particles were measured experimentally using a high-speed video camera and the NanoCrusher® (Micro Materials, UK), at the University of Leeds, respectively. The particle and simulation properties are summarised in Tables 1 and 2, where particle size follows a normal distribution.

2.2.1 Implementation of Clumped Spheres

X-ray tomography (XRT) is used to provide three-dimensional (3D) information on the granule structure. A Phoenix Nanotom© CT scanner (GE Measurement and Control, US) was

used to obtain the 3D structure of a single corn seed in the 7.1 – 8.0 mm sieve-cut, as shown in Figure 4, followed by the generation of clumped spheres by the ASG2013 software (Cogency, South Africa) as shown in Figure 5. In order to investigate the effect of accuracy of shape representation, the clumped spheres were generated using 5, 10, 15 and 20 spheres, with volume errors of 0.1, 0.3, 0.1 and 0.2%, respectively, compared to the actual volume of the scanned corn seed. The clumped spheres are generated by populating the geometry of the particle, obtained from XRT, with suitable spheres (the number of spheres is defined by the user) by means of a random selection process. Once the spheres are generated, an iterative optimisation process adjusts the solution until the distance between the mesh surface and the clumped spheres surface is minimised [24]. The number of spheres and amount of overlap used in the assembly controls the roughness of the particles, where the larger the number of spheres and overlap, the smoother the surface of the particle.

3 Results and Discussion

3.1 Experimental Particle Velocity Distributions

The measured radial and tangential velocity distributions of particles in the cell located after the baffle forming the bed surface are shown in Figures 6a and 6b, respectively, for 1250 particles over a period of 6 seconds (approximately 10,000 velocity samples). The total number of bins (11) and bin size that are used for generating the velocity distributions in this work are kept constant to aid the comparison. The radial and tangential velocity distributions of the particles have peak values at -0.55 and 0.39 m/s, respectively. The positive values in tangential and radial velocities indicate that the particles are moving anti-clockwise and towards the vessel wall, respectively.

3.2   Effect of the Rolling Friction Coefficient on Simulated Velocity Distributions

The predicted radial velocity distributions of spherical particles after the baffle are shown in Figure 7, where the rolling friction coefficient is varied from 0.01 to 0.3. The motion of particles is not sensitive to small values of rolling friction (i.e. $0.01 - 0.05$). Once the rolling friction value of 0.05 is exceeded, the motion of the particles becomes more sensitive to the selected value. In the case of the tangential velocity of the particles after the baffle (Figure 8), the peak and span of the distribution remain relatively constant when changing the particle-particle rolling friction coefficient, suggesting the tangential motion of the particles after the baffle is not influenced by varying the particle-particle rolling friction coefficient.

The predicted radial velocity distributions of spherical particles in the measurement cell located before the baffle are shown in Figure 9. It is clear that the radial motion of particles in this case is sensitive for the entire range of investigated values of rolling friction. The magnitude of the radial velocity corresponding to the mode of the distribution decreases as the rolling friction is increased. It is most unlikely that the contacts between the particles have a shear component, therefore an increase in the rolling friction restricts the particles from rolling on each other and hence reduces the particle velocity. However, looking at the tangential velocity distribution of particles located before the baffle, as shown in Figure 10, the motion of particles is not sensitive to values of rolling friction coefficient in the range of $0.01 - 0.1$. This suggests that using the current experimental setup (i.e. baffle angle and clearance gap), particles-particle rolling friction coefficient is more influential on the radial motion of the particles in the coater than the tangential motion.

Comparing the tangential velocity distribution of particles in the measurement cells located before and after the baffle, the motion of particles is more sensitive to the value of rolling

friction before the baffle than after. This is due to the fact that there are more inter-particle contacts before the baffle than after, as shown in Figure 11.

3.3   Clumped Spheres

The predicted radial velocity distributions of particles, as represented by a number of clumped spheres in the measurement cells located after and before the baffle, are shown in Figure 12. The radial velocity of the particles is almost independent of the number of spheres used (for 5 – 20 spheres). A similar trend is also obtained for the tangential velocity distribution of the particles, as shown in Figure 13. This clearly shows that the motion of particles is not sensitive to the number of spheres used to represent the particle shape in the DEM simulations of the seed coater in this study, as long as the general particle shape is represented. In this case five spheres was sufficient to represent the particle shape, however it remains to be seen if fewer clumped spheres can achieve this without the artificial use of the rolling friction. Moreover, the least number of clumped spheres can be used to accurately simulate this system in order to speed up the calculations.

3.4   Comparison of Experimental Results and Simulation Predictions

The effectiveness of both methods is investigated by comparing the simulation predictions and experimental results. As there is no change in the tangential and radial velocity of particles when the number of clumped spheres is increased, the experimental results are compared for the simplest case, where the seeds are represented by five clumped spheres. The radial and tangential velocity distributions of particles in the measurement cell located after the baffle are shown in Figure 14. In the case of radial velocity, the rolling friction coefficients of 0.01 and 0.3 provide a poor match to the experiments, whilst a rolling friction coefficient of 0.1 gives a reasonably good match. It can be seen that the DEM simulation of the seed coater using clumped spheres gives reasonably accurate prediction of the motion of

particles. However, there is a slight lack of agreement on smaller values of magnitude of radial velocity and larger values of tangential velocity of the particles. This could be due to the fact that some of the particles being tracked in the experiments were near the base of the coater; hence they tended to have larger tangential and smaller radial velocities. Moreover, it is clear that by using the rolling friction method, the motion of particles can be suitably simulated by DEM using a rolling friction coefficient of 0.1 (see the similarity between the velocity distributions using rolling friction coefficients 0.1 and experimental results in Figure 14). However, the value of this parameter is unknown a priori, so there is lack of predictability by this method.

It should be noted that the radial and tangential velocities of particles before the baffle could not be measured experimentally due to the complexity of particle motion. However, since the motion of particles is not sensitive to the number of clumped spheres after the baffle and the simulation parameters are measured experimentally without any calibration, an assumption can be made that the velocity distribution of the particles before the baffle using the clumped sphere method is representative of experiments. Based on this assumption, a rolling friction value between $0.05 - 0.1$ can be used in the DEM simulations of the seed coater to accurately represent the experimental behaviour as shown in Figure 15. Average radial and tangential velocities of 0.58 and 0.42 m/s, respectively, are obtained for both methods of particle shape representation, respectively; however, the span of the distribution is slightly larger for the rolling friction method than the clumped sphere method. With the methodology established here the next step of addressing the quality of mixing can be addressed confidently using the clumped sphere method.

4 Conclusions

The DEM results indicate that for simulating particle motion in rapid shear coaters, e.g. in the rotary batch seed coater investigated in this study, the motion of non-spherical particles can be simulated using clumped spheres or by controlling rolling friction. In the case of artificially changing the rolling friction of spherical particles, a reasonable agreement is found for both tangential and radial velocities for a narrow range of the chosen values. However, the motion of particles is slightly more sensitive to the value of rolling friction before the baffle, where there are more inter-particle contacts than after the baffle. It is also shown that the motion of particles can be predicted using the clumped sphere method. The number of spheres used to represent the particle shape is not critical for the range investigated. The work reported here suggests that clumped spheres provide a satisfactory representation of particle shape for rapid shearing systems with short collisional contacts. A small number of clumped spheres can provide a reasonable agreement with experimental results. Manipulating the rolling friction coefficient of single spheres can also provide results that closely match experiments to the clumped sphere method, but its most suitable value is unknown a priori, hence the approach is empirical rather than predictive.

Acknowledgements

References

[1] P. A. Cundall and O. D. L. Strack, "A Discrete Numerical Model for Granular Assemblies," Géotechnique, vol. 29, no. 1, pp. 47–65, Jan. 1979.

[2] P. W. Cleary, "DEM Prediction of Industrial and Geophysical Particle Flows," Particuology, vol. 8, no. 2, pp. 106–118, Apr. 2010.

[3] C. O'Sullivan, Particulate Discrete Element Modelling: A Geomechanics Perspective. Taylor & Francis, 2011.

[4] H. P. Zhu, Z. Y. Zhou, R. Y. Yang, and A. B. Yu, "Discrete Particle Simulation of Particulate Systems: A Review of Major Applications and Findings," Chem. Eng. Sci., vol. 63, no. 23, pp. 5728–5770, Dec. 2008.

[5] L. Rothenburg and R. J. Bathurst, "Numerical Simulation of Idealized Granular Assemblies with Plane Elliptical Particles," Comput. Geotech., vol. 11, no. 4, pp. 315–329, Jan. 1991.

[6] P. A. Cundall, "Formulation of a Three-Dimensional Distinct Element Model—Part I. A Scheme to Detect and Represent Contacts in a System Composed of Many Polyhedral Blocks," Int. J. Rock Mech. Min. Sci. Geomech. Abstr., vol. 25, no. 3, pp. 107–116, Jun. 1988.

[7] A. V. Potapov and C. S. Campbell, "A Three-Dimensional Simulation of Bittle Solid Fracture," Int. J. Mod. Phys. C, vol. 07, no. 05, pp. 717–729, Oct. 1996.

[8] L. Pournin, M. Weber, M. Tsukahara, J. a. Ferrez, M. Ramaioli, and T. M. Liebling, "Three-dimensional distinct element simulation of spherocylinder crystallization," Granul. Matter, vol. 7, no. 2–3, pp. 119–126, 2005.

[9] J. R. Williams and A. P. Pentland, "Superquadrics and Modal Dynamics for Discrete Elements in Interactive Design," Eng. Comput., vol. 9, no. 2, pp. 115–127, Feb. 1992.

[10] G. Lu, J. R. Third, and C. R. Müller, "Discrete element models for non-spherical particle systems: From theoretical developments to applications," Chem. Eng. Sci., vol. 127, pp. 425–465, 2015.

[11] J. K. Morgan, "Particle Dynamics Simulations of Rate- and State-Dependent Frictional Sliding of Granular Fault Gouge," Pure Appl. Geophys., vol. 161, no. 9–10, pp. 1877–1891, Aug. 2004.

[12] J. Ai, J.-F. Chen, J. M. Rotter, and J. Y. Ooi, "Assessment of Rolling Resistance Models in Discrete Element Simulations," Powder Technol., vol. 206, no. 3, pp. 269–282, Jan. 2011.

[13] C. M. Wensrich and A. Katterfeld, "Rolling Friction as a Technique for Modelling Particle Shape in DEM," Powder Technol., vol. 217, pp. 409–417, Feb. 2012.

[14] J. F. Favier, M. H. Abbaspour-Fard, M. Kremmer, and A. O. Raji, "Shape Representation of Axi-Symmetrical, Non-Spherical Particles in Discrete Element Simulation Using Multi-Element Model Particles," Eng. Comput., vol. 16, no. 4, pp. 467–480, 1999.

[15] J. F. Favier, M. H. Abbaspour-Fard, and M. Kremmer, "Modeling Nonspherical Particles Using Multisphere Discrete Elements," J. Eng. Mech., vol. 127, pp. 971–977, 2001.

[16] W. R. Ketterhagen, M. T. Am Ende, and B. C. Hancock, "Process Modeling in the Pharmaceutical Industry Using the Discrete Element Method.," J. Pharm. Sci., vol. 98, no. 20, pp. 442–470, 2009.

[17] J. Wiącek, M. Molenda, J. Horabik, and J. Y. Ooi, "Influence of Grain Shape and Intergranular Friction on Material Behavior in Uniaxial Compression: Experimental and DEM Modeling," Powder Technol., vol. 217, pp. 435–442, Feb. 2012.

[18] C. Hare and M. Ghadiri, "The Influence of Aspect Ratio and Roughness on Flowability," in Powders and Grains 2013, 2013, pp. 887–890.

[19] C. González-Montellano, Á. Ramírez, E. Gallego, and F. Ayuga, "Validation and Experimental Calibration of 3D Discrete Element Models for the Simulation of the Discharge Flow in Silos," Chem. Eng. Sci., vol. 66, no. 21, pp. 5116–5126, Nov. 2011.

[20] R. Balevičius, R. Kačianauskas, Z. Mróz, and I. Sielamowicz, "Discrete-Particle Investigation of Friction Effect in Filling and Unsteady/Steady Discharge in Three-dimensional Wedge-Shaped Hopper," Powder Technol., vol. 187, no. 2, pp. 159–174, Oct. 2008.

[21] C. González-Montellano, E. Gallego, Á. Ramírez-Gómez, and F. Ayuga, "Three Dimensional Discrete Element Models for Simulating the Filling and Emptying of Silos: Analysis of Numerical Results," Comput. Chem. Eng., vol. 40, pp. 22–32, May 2012.

[22] Z. Lu, S. C. Negi, and J. C. Jofriet, "A Numerical Model for Flow of Granular Materials in Silos . Part 1 : Model Development," pp. 223–229, 1997.

[23] Y. Song, R. Turton, and F. Kayihan, "Contact detection algorithms for DEM simulations of tablet-shaped particles," Powder Technol., vol. 161, no. 1, pp. 32–40, 2006.

[24] M. Price, V. Murariu, and G. Morrison, "Sphere clump generation and trajectory comparison for real particles," in Fourth International Conference on Discrete Element Methods (DEM), 2007.

[25] D. Markauskas, R. Kačianauskas, a. Džiugys, and R. Navakas, "Investigation of adequacy of multi-sphere approximation of elliptical particles for DEM simulations," Granul. Matter, vol. 12, no. 1, pp. 107–123, 2010.

[26] M. Kodam, R. Bharadwaj, J. Curtis, B. Hancock, and C. Wassgren, "Cylindrical object contact detection for use in discrete element method simulations, Part II-Experimental validation," Chem. Eng. Sci., vol. 65, no. 22, pp. 5863–5871, 2010.

[27] H. Kruggel-Emden, S. Rickelt, S. Wirtz, and V. Scherer, "A study on the validity of the multi-sphere discrete element method," Powder Technol., vol. 188, no. 2, pp. 153–165, Dec. 2008.

[28] Y. Guo, C. Wassgren, W. Ketterhagen, B. Hancock, B. James, and J. Curtis, "A numerical study of granular shear flows of rod-like particles using the discrete element method," J. Fluid Mech., no. July, pp. 1–26, 2012.

[29] H. R. Hertz, "Über die Berührung fester elastischer Körper," J. Reine Angew.Math, vol. 94, pp. 156–171, 1882.

[30] Y. C. Zhou, B. D. Wright, R. Y. Yang, B. H. Xu, and A. B. Yu, "Rolling Friction in the Dynamic Simulation of Sandpile Formation," Phys. A Stat. Mech. its Appl., vol. 269, no. 2–4, pp. 536–553, Jul. 1999.

[31] S. Lommen, D. Schott, and G. Lodewijks, "DEM speedup: Stiffness Effects on Behavior of Bulk Material," Particuology, vol. 12, pp. 107–112, Feb. 2014.

[32] R. Moreno-Atanasio, B. H. Xu, and M. Ghadiri, "Computer simulation of the effect of contact stiffness and adhesion on the fluidization behaviour of powders," Chem. Eng. Sci., vol. 62, no. 1–2, pp. 184–194, Jan. 2007.
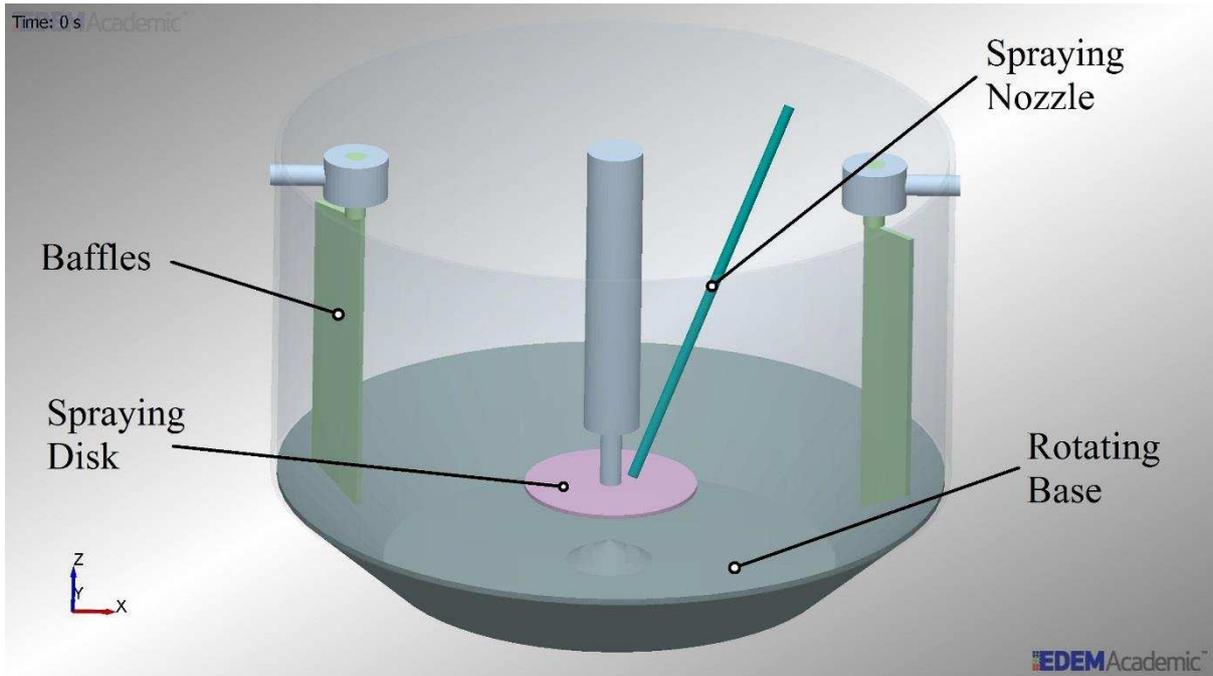
**Figure 1** Geometry of vertical rotating drum coater
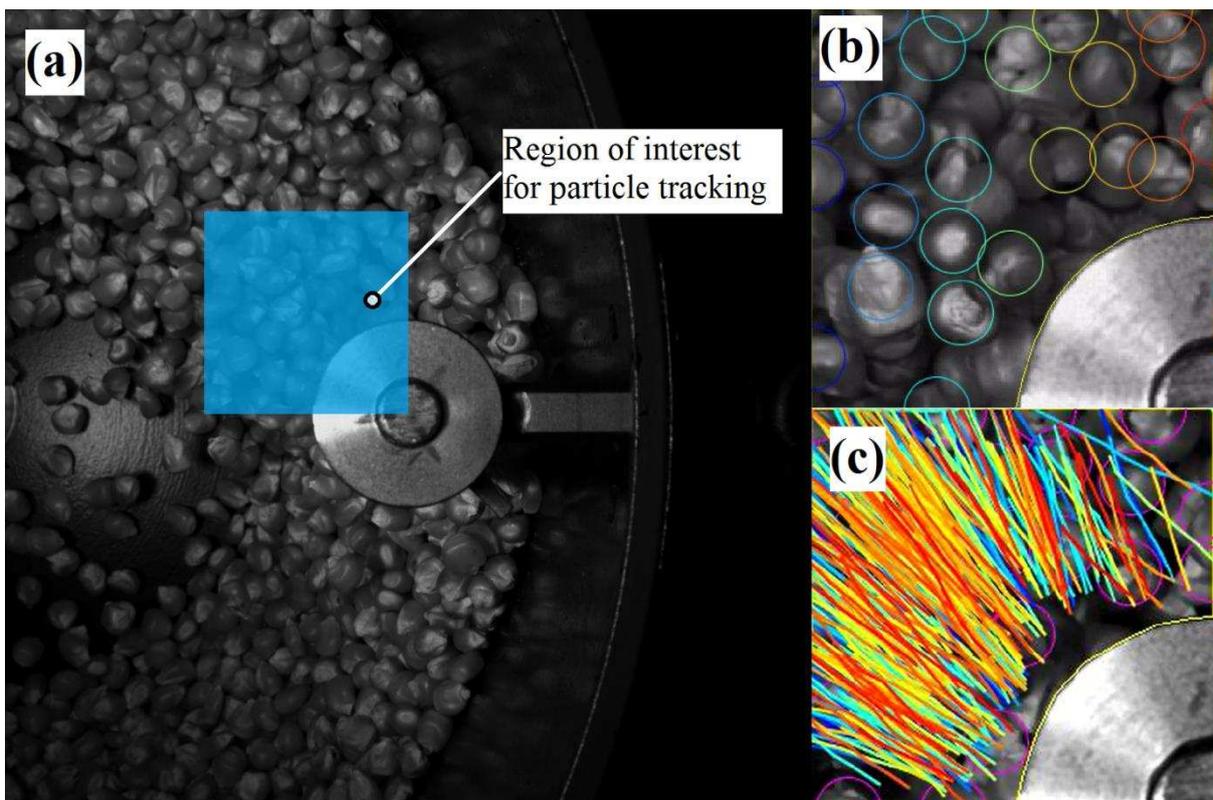
Figure 2 Particle tracking for obtaining tangential and radial velocity distributions of particles in the measurement cell located after the baffle; a) shows the region where the particle trajectories are analysed, b) detection of particles in the cell and c) is representation of track of the particles throughout the whole video
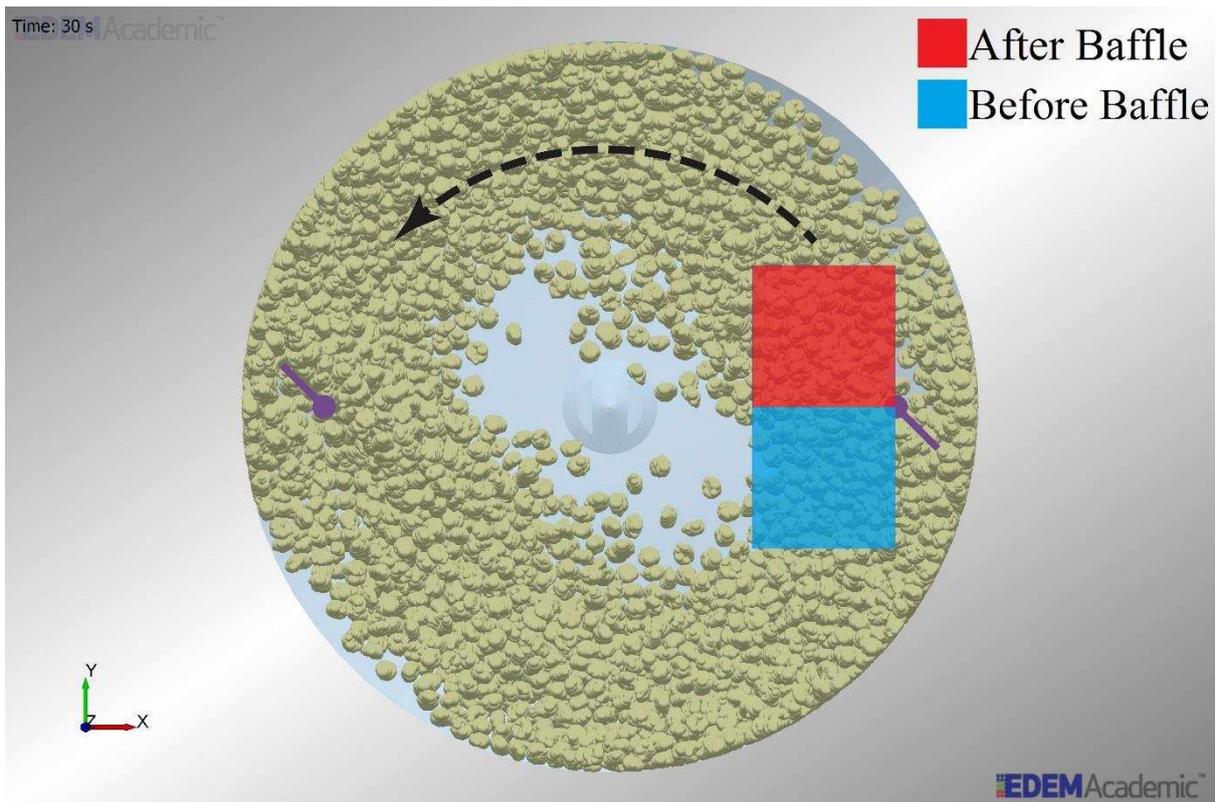
Figure 3 Measurement cells in DEM simulations for two positions in the vessel, one after (red) and another before (blue) the baffle
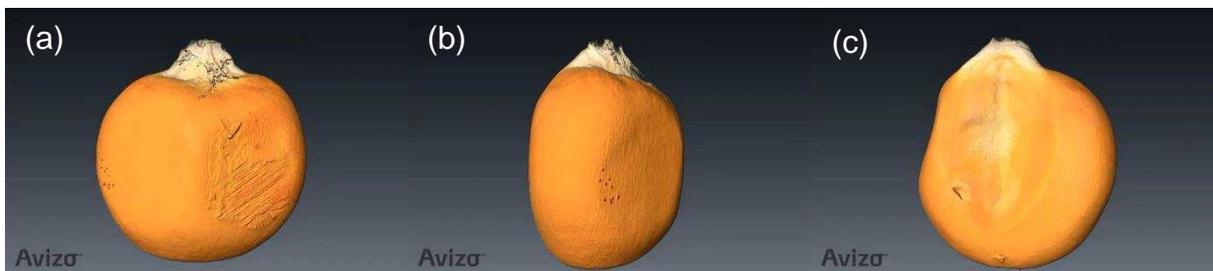
Figure 4 (Colour online) Three-dimensional structure of a corn seed obtained from XRT.
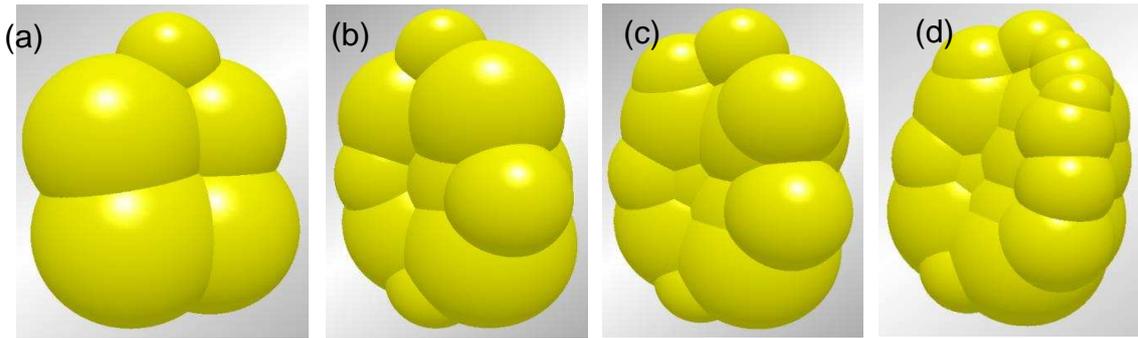
Figure 5 Representation of Corn Seeds in DEM using (a) five, (b) ten, (c) fifteen and (d) twenty spheres

(a)

(b)
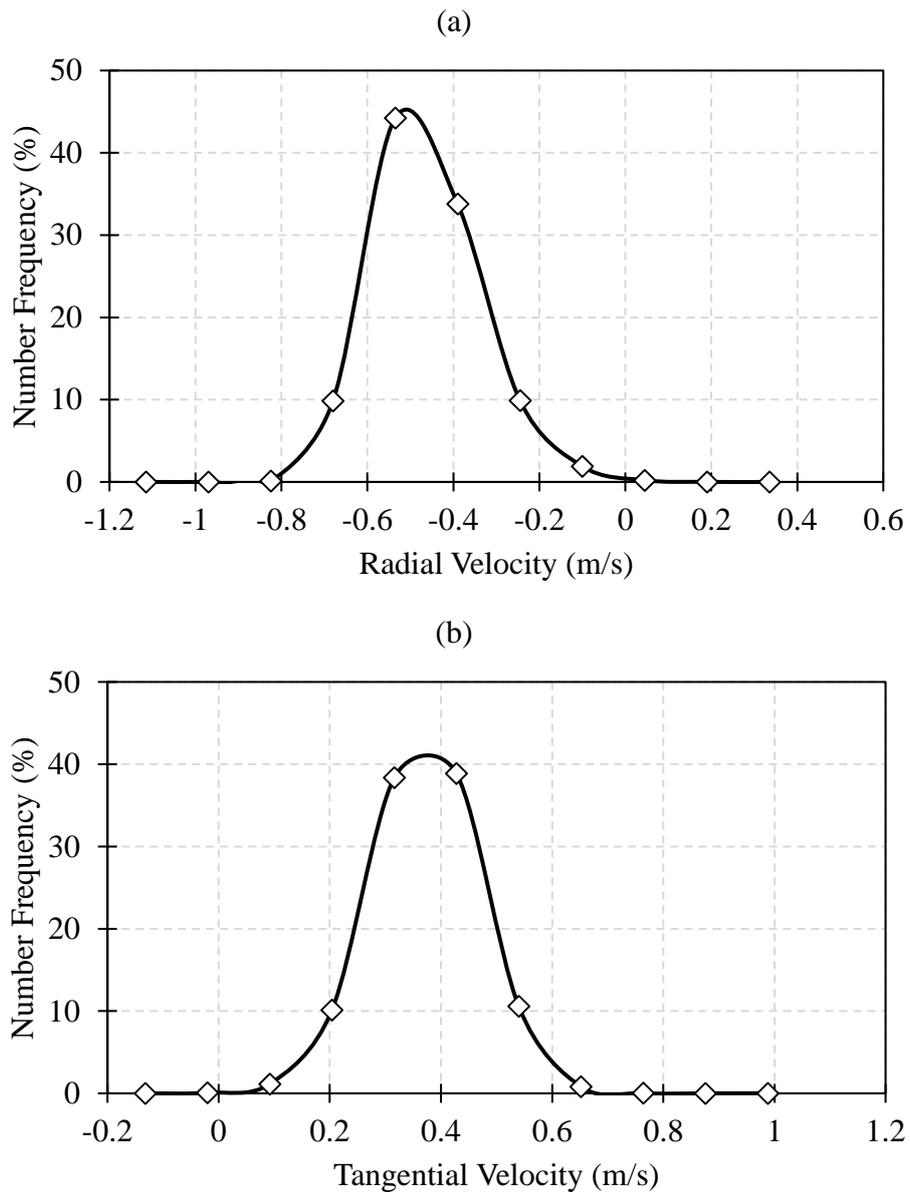
**Figure 6** Experimental tangential (a) and radial (b) velocity distributions in the measurement cell located after the baffle.
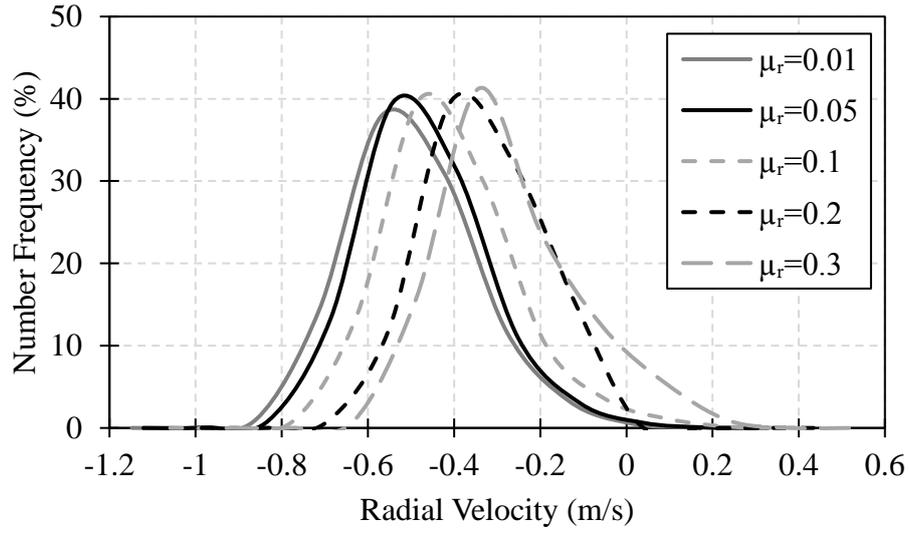
Figure 7 Predicted radial velocity distribution of particles in the measurement cell located after the baffle using rolling friction method
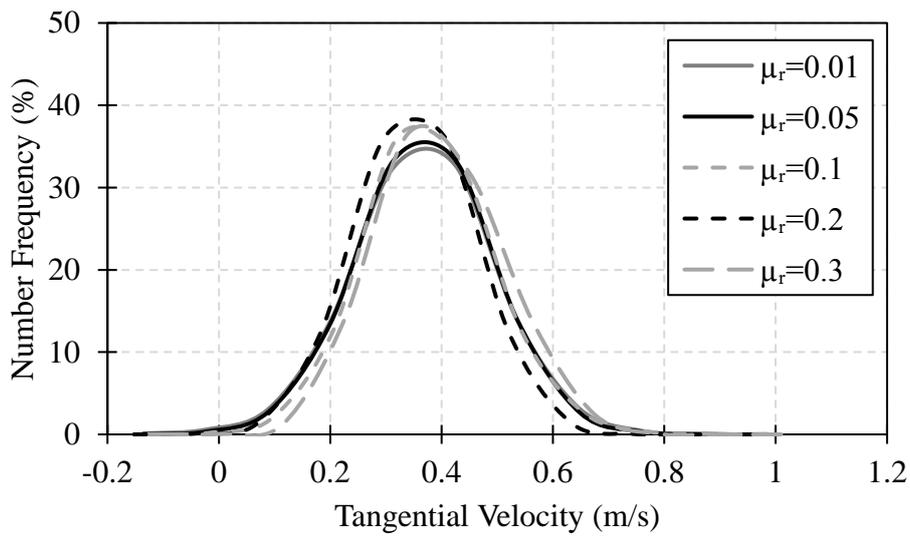

Figure 8 Predicted tangential velocity distribution of particles in the measurement cell located after the baffle using rolling friction method
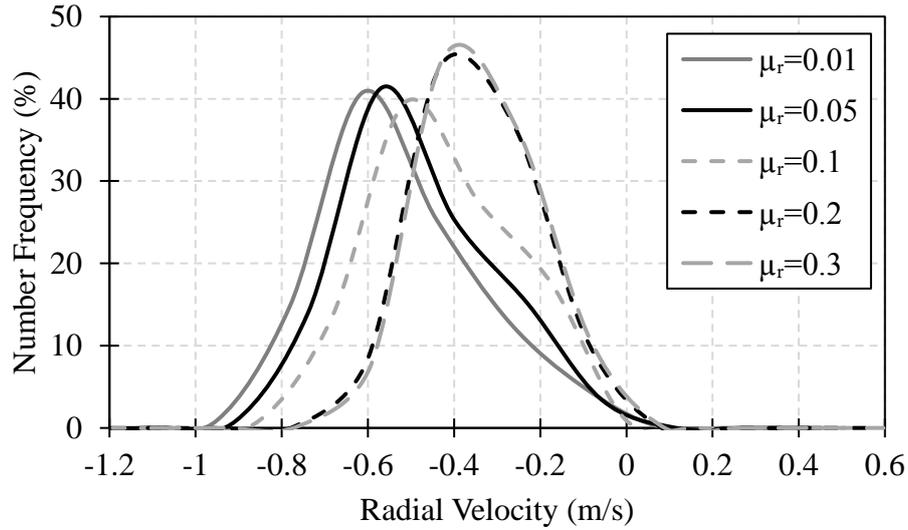
Figure 9 Predicted radial velocity distribution of particles in the measurement cell located before the baffle using rolling friction method
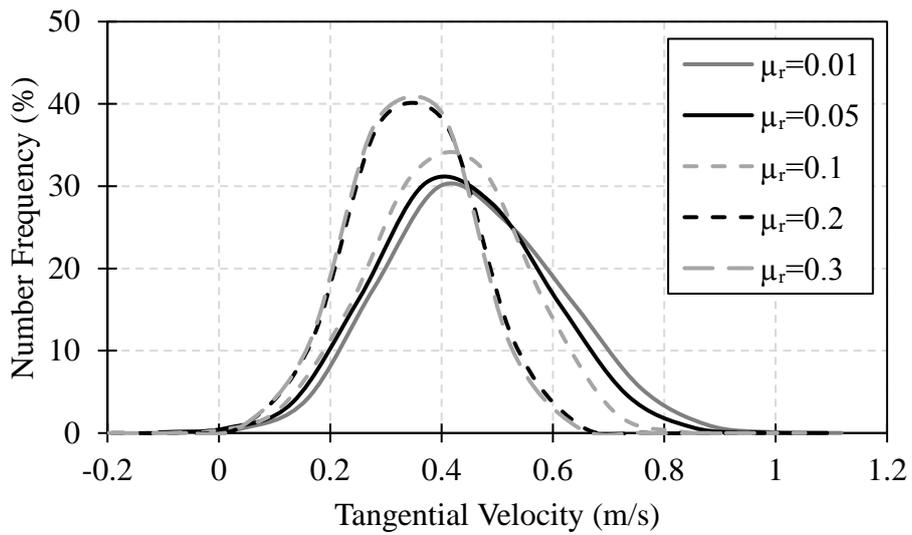
Figure 10 Predicted tangential velocity distribution of spherical particles in the measurement cell located before the baffle using rolling friction method
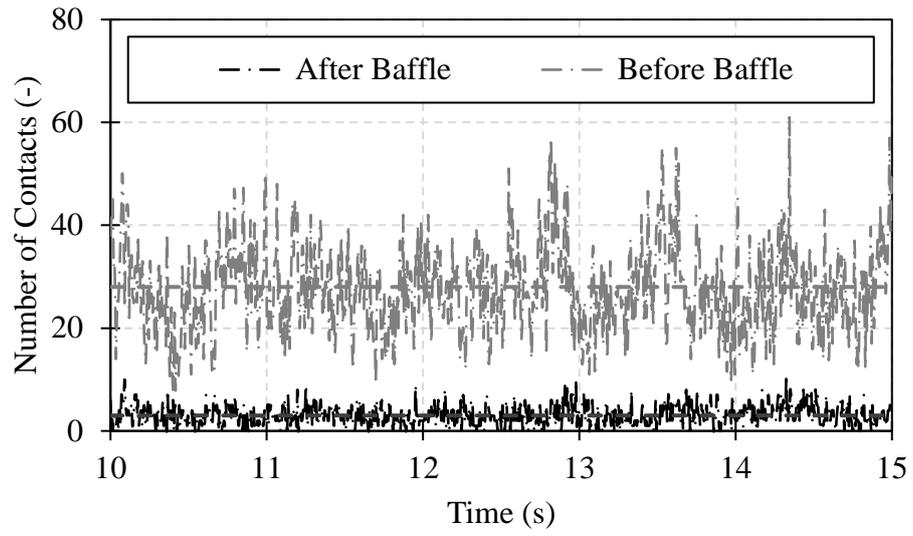
Figure 11 Comparison of number of inter-particle contacts in the measurement cells located after and before the baffle for the simulation of rolling friction coefficient of 0.1.

(a)

(b)
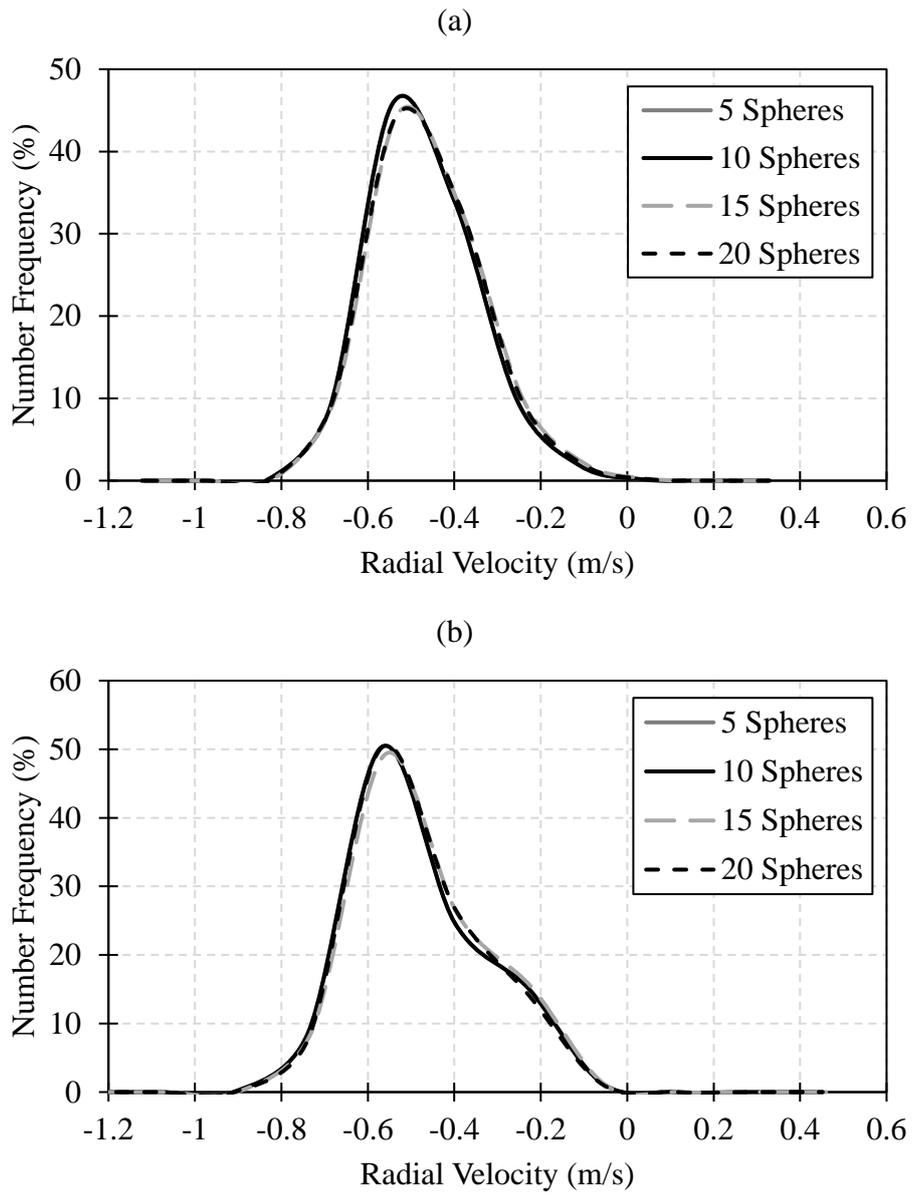
Figure 12 Predicted tangential velocity distributions of particles in the measurement cells located (a) after and (b) before the baffle using the overlapping spheres method

(a)

(b)
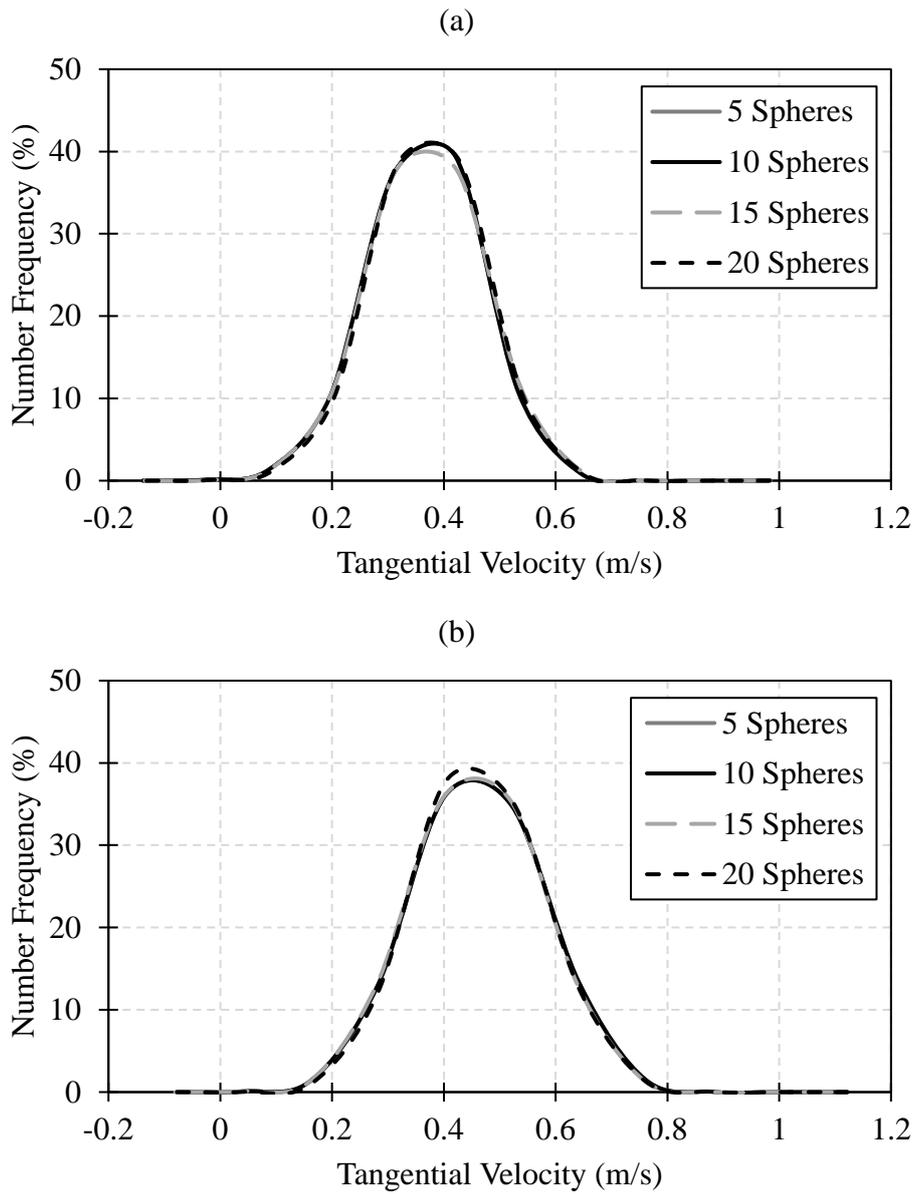
Figure 13 Predicted radial velocity distribution of particles in the measurement cell located (a) before and (b) after the baffle using the overlapping sphere method

24
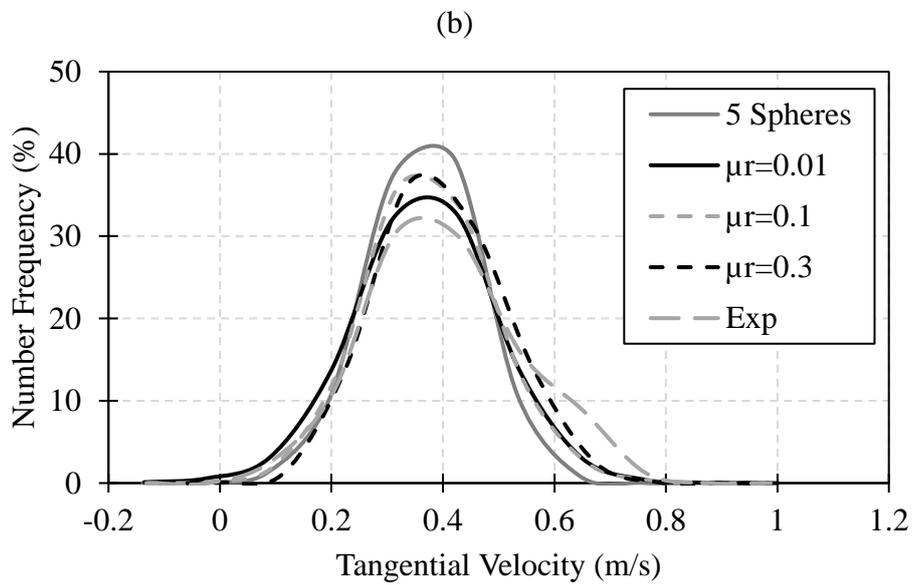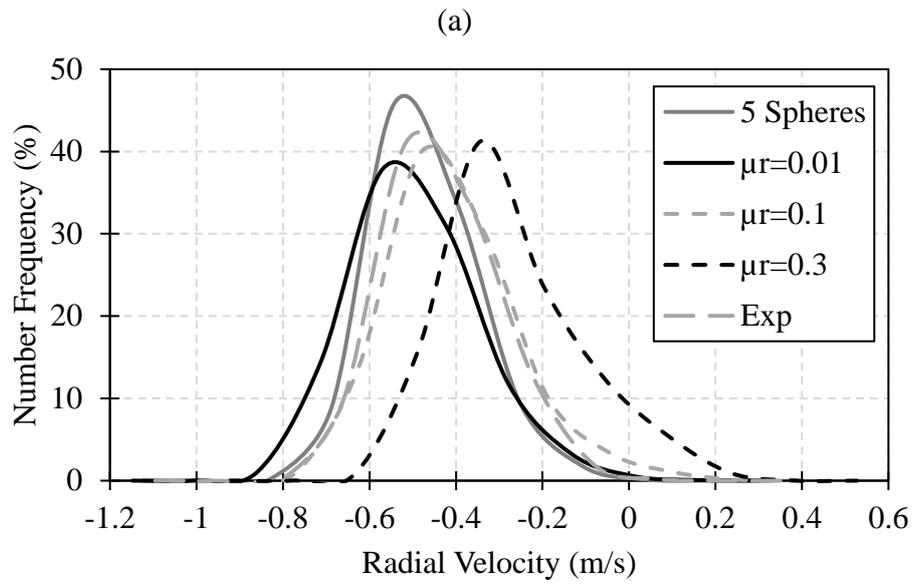
Figure 14 Comparison of experimental results and simulation predictions for the measurement cell located after the baffle: (a) radial velocity; (b) tangential velocity
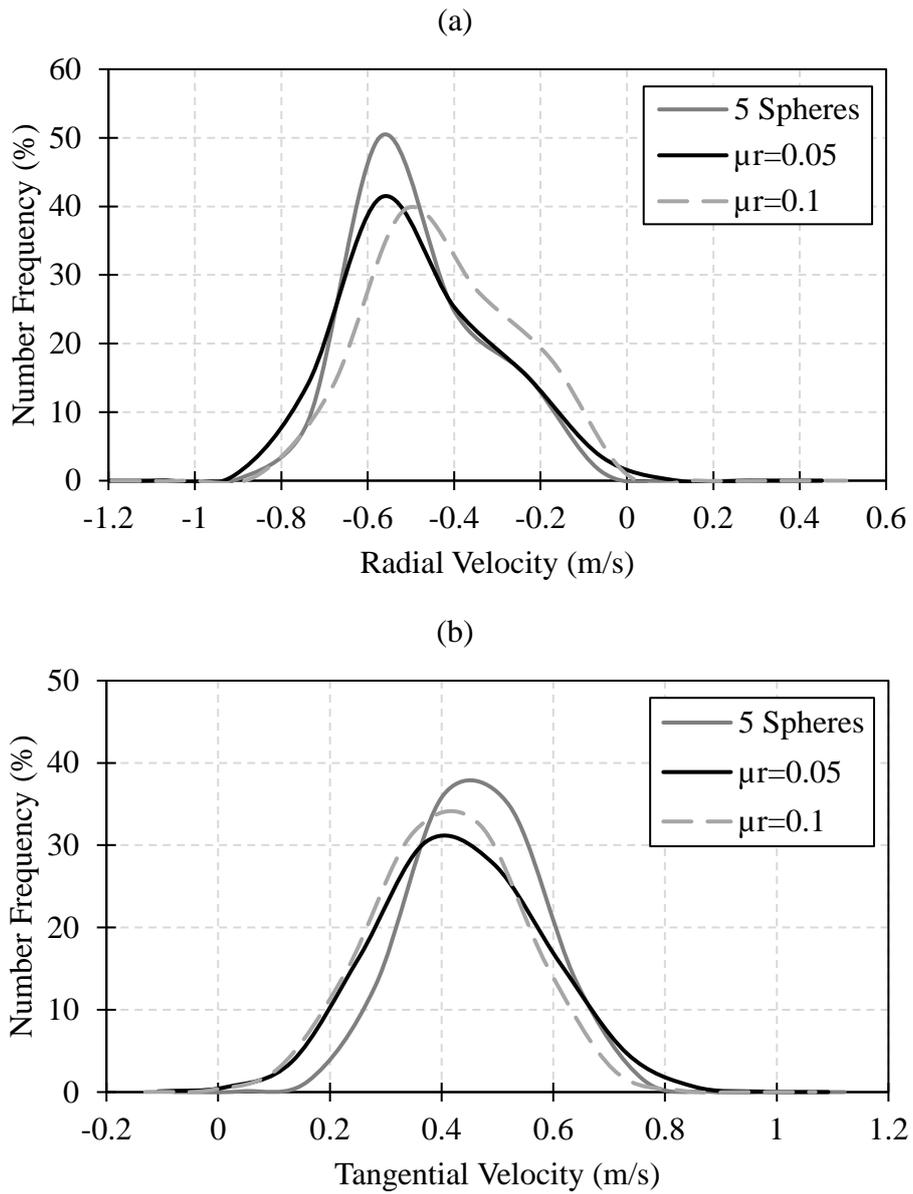
Figure 15 Comparison of tangential and radial velocity distribution of particles using clump sphere and rolling friction methods in DEM simulations: (a) radial velocity; (b) tangential velocity

Table 1 Properties of particles and walls used in DEM simulations

Property	Seeds	Walls (steel)
Particle diameter (mm)	$7.5 \pm 3\%$	-
Shear Modulus (GPa)	0.01	70
Density (kg/m^3)	1163	7800
Poisson's Ratio (-)	0.25	0.3

Table 2 Contact properties used in DEM simulations

Property	Particles-Particle	Particle-Wall
Coefficient of Sliding Friction	0.3	0.3
Coefficient of Rolling Friction[*]	0.01 – 0.3	0.01
Coefficient of Restitution	0.6	0.69

[*]Using the model of Zhou et al. [29]